

RESEARCH ARTICLE | MARCH 01 1968

## Raman Spectrum of Strontium Titanate

W. G. Nilsen; J. G. Skinner



*J. Chem. Phys.* 48, 2240–2248 (1968)

<https://doi.org/10.1063/1.1669418>



### Articles You May Be Interested In

Electronic Absorption Spectra of Methanal Azine and the Methyleniminyl Free Radical

*J. Chem. Phys.* (March 1968)

Raman Spectrum of Potassium Tantalate

*J. Chem. Phys.* (August 1967)

Infrared-Absorption Spectrum and Ferroelectric Behavior of Sodium Trihydroselenite

*J. Chem. Phys.* (November 1965)



Nanotechnology &  
Materials Science



Optics &  
Photonics



Impedance  
Analysis



Scanning Probe  
Microscopy



Sensors



Failure Analysis &  
Semiconductors



Unlock the Full Spectrum.  
From DC to 8.5 GHz.

Your Application. Measured.

[Find out more](#)



# Raman Spectrum of Strontium Titanate

W. G. NILSEN AND J. G. SKINNER

*Bell Telephone Laboratories, Incorporated, Murray Hill, New Jersey*

(Received 19 September 1967)

The Raman spectrum of single-crystal  $\text{SrTiO}_3$  has been investigated as a function of temperature down to about 25°K. The lattice dynamics of this crystal have been extensively studied in recent years primarily because of its unusual dielectric and acoustic properties. Both nominally pure and impure samples were examined since these properties seem to be sensitive to small amounts of impurities. An argon-ion laser served as the exciting source and an in-tandem grating spectrometer was used to disperse the scattered light. These instrumental techniques provided rather complete data including the polarization characteristics of the individual lines and peaks. The above data, together with the known phonon dispersion curves of  $\text{SrTiO}_3$ , made it possible to obtain a reliable interpretation of the Raman spectrum. At room temperature we find the Raman spectrum to be entirely second order, in agreement with the selection rules for the cubic perovskite structure. Further, the phonons contributing to the second-order scattering have wave vectors at or near the Brillouin zone boundary and are for the most part transverse polarized. The same combinations and overtones tend to give intense peaks in both  $\text{SrTiO}_3$  and  $\text{KTaO}_3$ , but the different dispersions of the phonon branches in the two crystals make their spectra appear different. On cooling nominally pure  $\text{SrTiO}_3$  below the phase transition at 110°K, three sharp lines appear in the spectrum which are due to scattering from local modes rather than from the polar transverse-optic modes. The energy shifts measured for these three sharp lines do not agree with those for the polar TO modes. In the impure sample at low temperature (15°K) scattering from local modes and the polar transverse-optic modes are observed simultaneously. Measurements on the impure sample at 78°K yield scattering from the three polar transverse-optic modes but not from the local modes. These results illustrate the great sensitivity of Raman scattering to crystal structure and show that pure and impure  $\text{SrTiO}_3$  undergo different phase transitions as the temperature is reduced. Since no ferroelectricity or first-order Raman scattering is found in the tetragonal phase of pure  $\text{SrTiO}_3$ , the point group of this phase is most probably  $C_{4h}$  or  $D_{4h}$ . If the impure sample is tetragonal at 78°K, as is likely the case, then the Raman measurements show the point group to be  $S_4$ ,  $C_4$ , or  $C_{4v}$ . At lower temperatures the crystal structure is undoubtedly of lower symmetry than tetragonal.

## INTRODUCTION

Single-crystal  $\text{SrTiO}_3$  has been the subject of much study in recent years primarily because of its unusual dielectric and acoustic behavior. In order to achieve a better understanding of this unusual behavior, the lattice dynamics, crystal structure and possible phase transitions of  $\text{SrTiO}_3$  have been investigated extensively by a variety of methods. Using neutron-diffraction methods, Cowley<sup>1</sup> has obtained fairly complete data on the energy-vs-wave vector dispersion curves of the vibrational branches in  $\text{SrTiO}_3$  and compared these results with calculated dispersion curves using several lattice models. He also observed<sup>1,2</sup> that near the Brillouin zone center the lowest-energy transverse optic (ferroelectric) mode decreased in energy as the temperature was reduced, in agreement with the predictions of Cochran<sup>3</sup> and Anderson.<sup>4</sup> Neutron-diffraction studies yield a wealth of information on the energy of the phonon modes throughout the Brillouin zone but are not very sensitive to crystal symmetry or changes in crystal structure.

The lattice dynamics of  $\text{SrTiO}_3$  have also been studied by infrared techniques. These measurements yield the energies of the polar transverse optic (TO) modes near the Brillouin zone center. Both Barker and

Tinkham,<sup>5</sup> as well as Spitzer *et al.*,<sup>6</sup> measured the energy of the three active TO modes and observed that the energy of the ferroelectric mode decreased as the temperature was reduced. More recent and more extended analysis of the infrared data has yielded quite accurate energies not only for the polar TO modes<sup>7</sup> but also for the polar LO modes<sup>8</sup> at the zone center.

The Raman spectrum of  $\text{SrTiO}_3$  has also been studied extensively.<sup>9</sup> These studies have not added much to our understanding of the crystal dynamics of  $\text{SrTiO}_3$ , principally because of the difficulty in interpreting the Raman spectrum. These early studies were carried out with conventional light sources and spectrometers so that much of the data on polarization as well as the spectrum near the exciting line could not be obtained. In the present paper we describe some Raman experiments in which an argon-ion laser was used as the source and a double-pass spectrometer was used to disperse the scattered light. The improved Raman data have lead to a more complete interpretation of the spectrum.

It is useful here to give a short summary of the crystal properties of  $\text{SrTiO}_3$ . At room temperature the crystal has an ideal perovskite structure with one formula unit per unit cell. The dielectric constant is

<sup>5</sup> A. S. Barker, Jr., and M. Tinkham, *Phys. Rev.* **125**, 1527 (1962).

<sup>6</sup> W. G. Spitzer, R. C. Miller, D. A. Kleinman, and L. E. Howard, *Phys. Rev.* **126**, 1710 (1962).

<sup>7</sup> A. S. Barker, Jr., and J. J. Hopfield, *Phys. Rev.* **135**, A1732 (1964).

<sup>8</sup> A. S. Barker, Jr., *Phys. Rev.* **145**, 391 (1966).

<sup>9</sup> P. S. Narayanan and K. Vedam, *Z. Physik* **163**, 158 (1961).

<sup>1</sup> R. A. Cowley, *Phys. Rev.* **134**, A981 (1964).

<sup>2</sup> R. A. Cowley, *Phys. Rev. Letters* **9**, 159 (1962).

<sup>3</sup> W. Cochran, *Advan. Phys.* **9**, 387 (1960).

<sup>4</sup> P. W. Anderson, in *Fizika dielektrikov*, G. I. Skanavi, Ed. (Akademika Nauk SSSR Fizicheskii Inst. m P. N. Lebedeva, Moscow, 1960).

roughly 250 at room temperature but increases rapidly as the temperature is reduced.<sup>10-12</sup> The Curie-Weiss law is obeyed down to about 50°K with an extrapolated Curie temperature<sup>13</sup> of 38°K. Below 50°K the dielectric constant continues to rise but not fast enough to obey the Curie-Weiss law. Smolenskii<sup>12</sup> reports that a peak in the dielectric constant occurs at about 20° to 30°K, whereas Hulm<sup>10</sup> and Weaver<sup>11</sup> observed no peak down to 1.4°K. Small amounts of impurities undoubtedly have a large effect on the dielectric properties and lattice dynamics of SrTiO<sub>3</sub>.

The acoustic properties of SrTiO<sub>3</sub> have also been studied extensively both at room temperature<sup>14,15</sup> and at lower temperatures.<sup>16</sup> At room temperature the acoustic properties of SrTiO<sub>3</sub> are in accord with its cubic symmetry. As the temperature decreases, the elastic stiffness constants increase smoothly down to 108°K. At this temperature the ultrasonic attenuation abruptly increases and the elastic constants are greatly altered. This behavior indicates that a phase transition takes place at 108°C. Since no hysteresis effects are observed, the phase transition is probably second order or higher.<sup>16</sup>

Further evidence for a phase transition at about 110°K was obtained from electron paramagnetic resonance (EPR) studies of SrTiO<sub>3</sub> containing small amounts of paramagnetic ions.<sup>16-18</sup> Indeed, Müller first established that SrTiO<sub>3</sub> is tetragonal at low temperature from such studies. Rimai and deMars measured the EPR spectrum of Gd<sup>3+</sup> in SrTiO<sub>3</sub> as a function of temperature down to 1.5°K. With the magnetic field parallel to the [100] direction, the Gd<sup>3+</sup>-doped SrTiO<sub>3</sub> exhibited a spectrum expected of a cubic crystal down to about 110°K. Below this temperature the magnetic field for resonance changes abruptly for some transitions and an additional Gd<sup>3+</sup> spectrum appears. The former is due to the change of spin-Hamiltonian parameters from one consistent with cubic site symmetry to one consistent with tetragonal site symmetry. The latter indicates that the tetragonal domains are oriented along any of the original [100] directions, some of which are parallel and some perpendicular to the applied magnetic field. No spin-Hamiltonian terms were found which would indicate a rhombic distortion in the tetragonal phase. Microscopic examination<sup>19,20</sup> of

the domains in SrTiO<sub>3</sub> at liquid-nitrogen temperatures also indicates a tetragonal structure. Lytle, using x-ray diffraction methods, observed phase transitions at 65° and 35°K in addition to the cubic-tetragonal transition at 110°K, but these phase transitions have not been detected by other methods and may be due to crystal impurities.

The present evidence indicates that pure SrTiO<sub>3</sub> is cubic at room temperature, undergoes a second- (or higher-) order phase transition at about 110°K into one of the tetragonal point groups (possibly one of the nonferroelectric point groups), and does not undergo any further phase transitions down to 1.5°K. In impure SrTiO<sub>3</sub>, additional phase transitions may take place and the phase below 110°K may not have the same structure as in the pure crystal. We shall take advantage of this fact in our Raman studies described below.

## EXPERIMENTAL

The Raman experiments were carried out with an argon-ion laser and an in-tandem grating spectrometer. The experimental setup was described in an earlier paper.<sup>21</sup> Both the 4880- and 5145-Å laser lines were used in various experiments. Only right-angle scattering was investigated. The samples were oriented by standard x-ray techniques and placed in the apparatus so that the laser beam was directed along one [100] direction and the collected scattered light traveled parallel to another [100] direction. A half-wave plate was used to rotate the plane of polarization of the laser beam either parallel to the collected scattered light or the third [100] direction. The scattered light was analyzed with a polarizing sheet placed in front of the entrance slit. The low-temperature experiments were carried out in a helium cold-finger Dewar.

Several samples of SrTiO<sub>3</sub> were investigated. Crystals grown by flame fusion were nearly colorless and of sufficiently low strain so that the laser beam was depolarized only slightly (about 10%). Another sample was solution grown and brownish in color. This sample absorbed some laser radiation but still yielded a Raman spectrum.

## RESULTS

The Raman spectrum of the clear SrTiO<sub>3</sub> crystals grown by the flame fusion method is given in Figs. 1 and 2 for the crystal orientation described above. Both laser beam and detected scattered light were polarized perpendicular to the plane containing the laser beam and the entrance slit of the spectrometer. This polarization arrangement measures the diagonal elements of the scattering tensor. The nondiagonal elements are either zero or of much smaller magnitude (less than 10% of the diagonal elements). Figure 1 shows the complete spectrum as far as we have been

<sup>10</sup> J. K. Hulm, Proc. Phys. Soc. (London) **63**, 1184 (1950).

<sup>11</sup> H. E. Weaver, J. Phys. Chem. Solids **11**, 274 (1959).

<sup>12</sup> G. A. Smolenskii, Dokl. Akad. Nauk SSSR, Zh. Tekh. Fiz. **20**, 137 (1950).

<sup>13</sup> H. Gränicher, Helv. Phys. Acta **29**, 211 (1956).

<sup>14</sup> E. Poindexter and A. A. Giardini, Phys. Rev. **110**, 1069 (1958).

<sup>15</sup> J. B. Wachtman, Jr., M. L. Wheat, and S. Marzullo, J. Res. Natl. Bur. Std. **67A**, 193 (1963).

<sup>16</sup> K. A. Müller, Phys. Rev. Letters **2**, 341 (1959), Helv. Phys. Acta **31**, 173 (1958).

<sup>17</sup> W. I. Dobrov, R. F. Vieth, and M. E. Browne, Phys. Rev. **115**, 79 (1959).

<sup>18</sup> L. Rimai and G. A. deMars, Phys. Rev. **127**, 702 (1962).

<sup>19</sup> E. Sawaguchi, A. Kikuchi, and Y. Kodera, J. Phys. Soc. Japan **18**, 459 (1963).

<sup>20</sup> F. W. Lytle, J. Appl. Phys. **35**, 2212 (1964).

<sup>21</sup> W. G. Nilsen and J. G. Skinner, J. Chem. Phys. **47**, 1413 (1967).

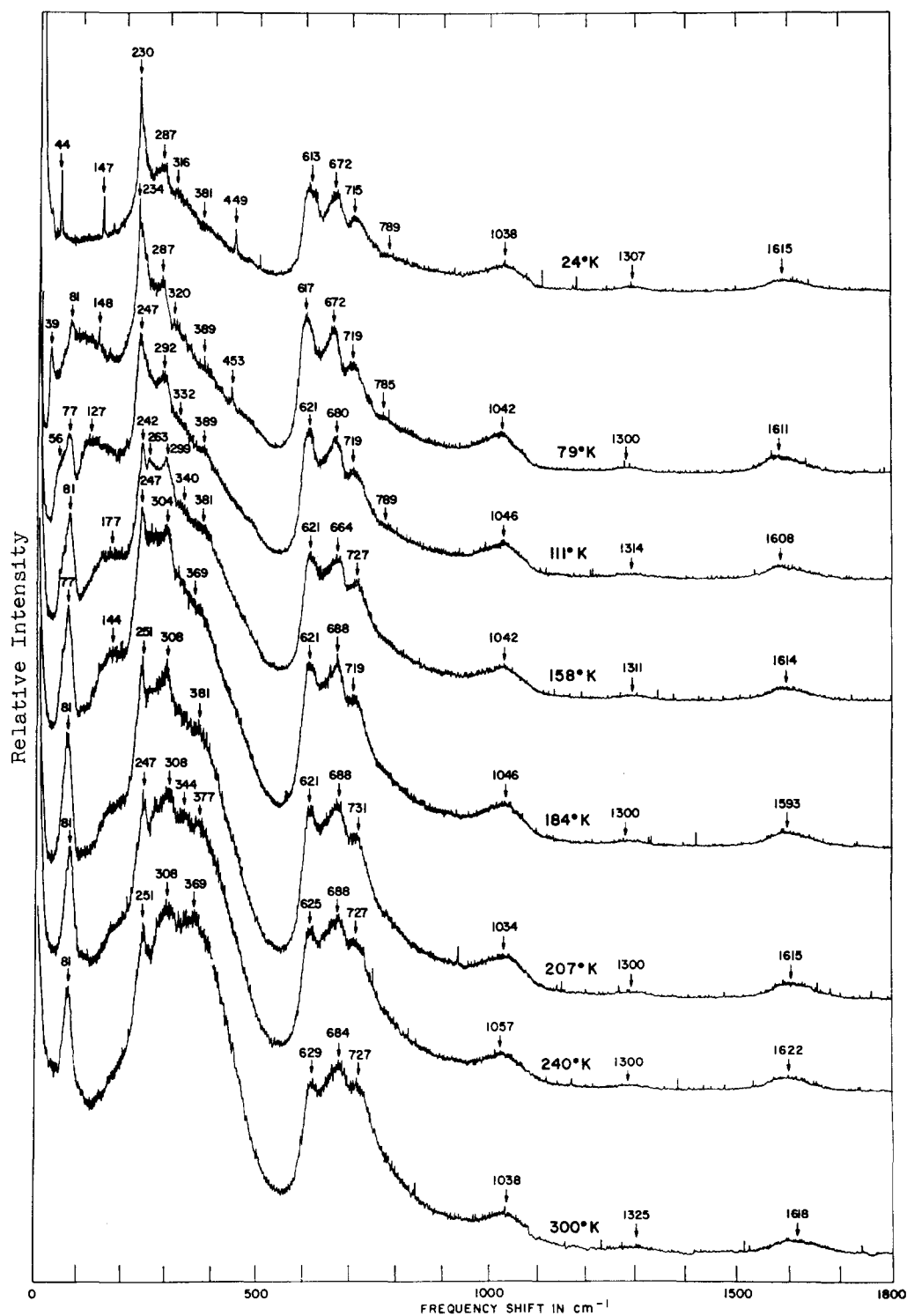


FIG. 1. The Raman spectrum of pure SrTiO<sub>3</sub> as a function of temperature using the 4880-Å laser line. The scale is approximate but the numbers marking various peaks are taken from a calibrated scan.

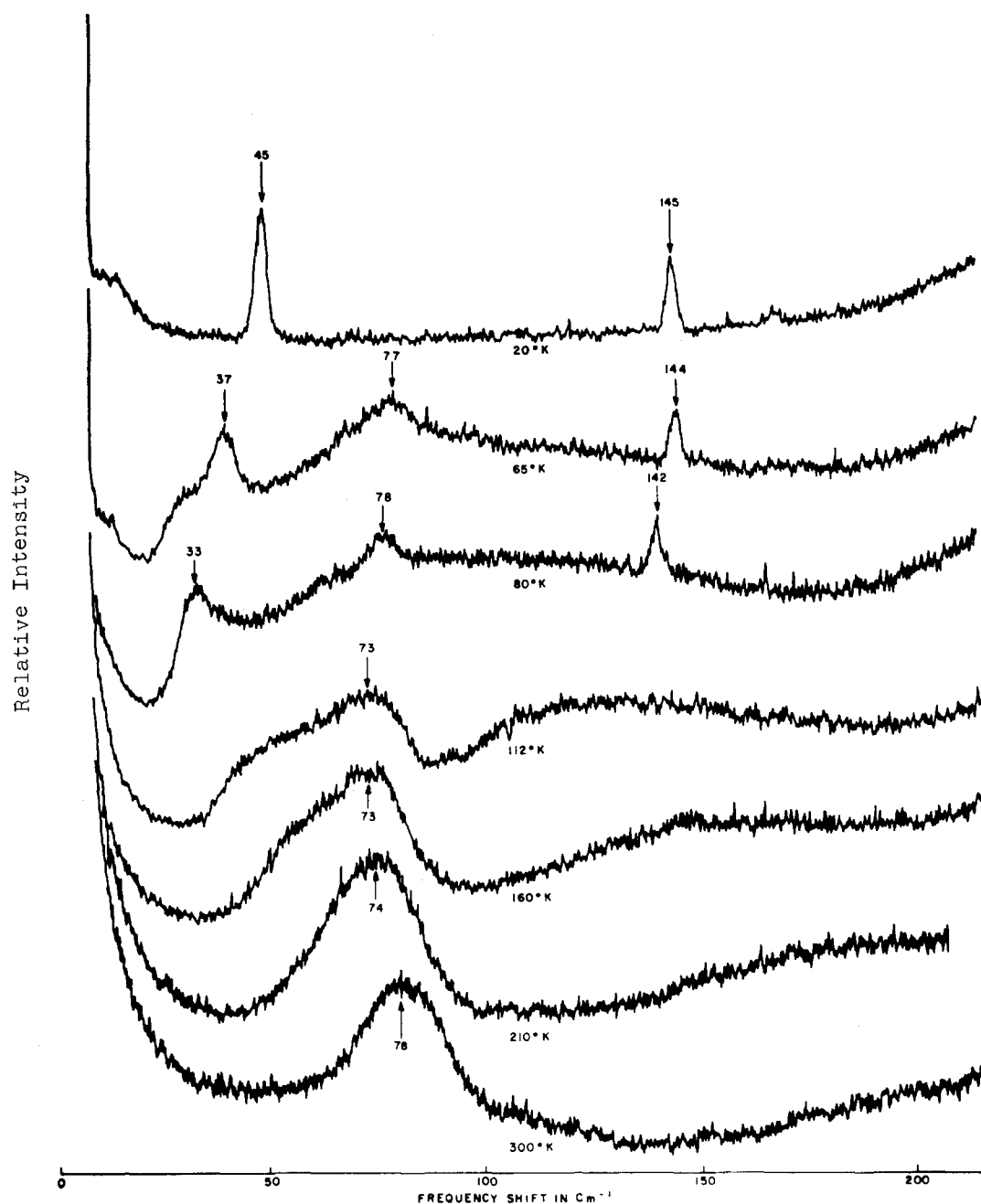


FIG. 2. Same as Fig. 1 except the scale has been expanded in order to show greater detail around the exciting line.

able to detect. The spectra in Fig. 2 were run with a slower scan speed in order to show more detail near the exciting line.

As the temperature is reduced below 110°K, three sharp lines appear in the spectrum which have energy shifts of 39, 148, and 453  $\text{cm}^{-1}$  at 79°K (see Fig. 1). These lines undoubtedly appear as a result of the phase transition at 110°K and are essentially unaltered, except for becoming sharper, as the temperature is lowered to 24°K.

Similar measurements were carried out on the

brownish sample grown from solution. The same crystal orientation was used. The results at room temperature duplicated those obtained from the clear sample. On cooling the sample to liquid-nitrogen temperatures, three additional sharp lines appear (see Fig. 3) as in the case of the clear samples but the energy shifts are significantly different. At lower temperatures around 15°K, three additional lines appeared whose energy shifts were approximately the same as found for the clear sample at low temperatures. All of the lines have only diagonal elements in their

scattering matrix. It is clear that the two samples undergo different structural changes as the temperature is reduced.

## DISCUSSION

### Second-Order Spectrum

Strontium titanate at room temperature has an ideal cubic perovskite structure with space group  $Pm\bar{3}m$  ( $O_h^1$ ). There are five atoms per unit cell, each of which is located at a point of inversion symmetry. At the Brillouin zone center, the 15 degrees of freedom are made up of one  $F_{1u}$  triply degenerate acoustic mode and three  $F_{1u}$  plus one  $F_{2u}$  triply degenerate optical modes.

In polar optical modes the energy degeneracy is removed even at the zone center because of the macroscopic electric-field effect associated with the polar longitudinal optic (LO) modes.<sup>22</sup> For this reason, the LO vibrational modes are found at a higher energy than the transverse optic (TO) modes derived from the same  $F_{1u}$  species. Also, the scattering cross section of the LO and TO modes belonging to the same species can be quite different<sup>22,23</sup> and depend on crystal orientation in different ways.

In the cubic phase neither the  $F_{1u}$  nor  $F_{2u}$  modes are Raman active, and no first-order Raman lines are expected at room temperature. Several previous attempts<sup>9,24</sup> to interpret the Raman spectrum of  $\text{SrTiO}_3$  at room temperature have assumed the spectra to be first order. We find the spectra of both  $\text{SrTiO}_3$  at room temperature<sup>21</sup> and  $\text{KTaO}_3$  to be entirely second order.

Second-order Raman spectra involve the creation or destruction of two phonons. In the case of Stokes components, overtone bands are obtained from the creation of two phonons from the same vibrational branch, addition combination bands from the creation of two phonons from different branches, and difference combination bands from the creation of one phonon and destruction of another phonon of lower energy. The anti-Stokes components are obtained by interchanging the roles of creation and destruction processes.

In first-order Raman processes, the phonon can only originate from a point near the zone center. The photon wave vectors are quite small compared to the width of the Brillouin zone and, therefore, the phonon wave vector must be small to conserve momentum. In second-order Raman processes, two phonons are available for momentum conservation so that the phonons can originate anywhere in the Brillouin zone provided their wave vectors add up to approximately zero.

Because of this difference in satisfying momentum conservation, first-order spectra are made up of discrete lines from individual branches in the vibrational spectrum, whereas the second-order spectra tend to be continuous. The structural details in second-order spectra are usually due to variations in the combined density of states, the selection rules, and the scattering intensities for individual points in the Brillouin zone.

Detailed selection rules have not been derived for second-order processes in the perovskite structure. For a general wave vector in the Brillouin zone, all overtones and combinations are allowed in crystals which have inversion symmetry. Our interpretation of the second-order spectra will be in terms of phonon energies near the zone boundary since at this point the density of states becomes quite large.

In Table I we give our assignment of the peaks in the room-temperature Raman spectrum of  $\text{SrTiO}_3$ . The peaks are identified by their room-temperature energy shifts given in Fig. 1. Since our interpretation leans heavily on our results for  $\text{KTaO}_3$ , we give the energy shifts for the corresponding Raman peaks in this crystal. In order to distinguish overtones and addition combination bands from difference combination bands, the Raman spectrum was also measured at several temperatures below room temperature. The difference combination band should decrease in intensity relative to the other bands.<sup>25</sup> For example, the band at  $81\text{ cm}^{-1}$  is obviously a difference combination band since its intensity approaches zero as the temperature is lowered toward  $0^\circ\text{K}$ . In contrast, the band at  $251\text{ cm}^{-1}$  does not decrease in intensity as the temperature is reduced and must be either an overtone or addition combination band. We assign the  $81\text{-cm}^{-1}$  band to the  $\text{TO}_2\text{--TA}$  and  $\text{TO}_2\text{--TO}_1$  combinations and the  $251\text{-cm}^{-1}$  band to the overtones  $2\text{TA}$  and  $2\text{TO}_1$  and the addition combination  $\text{TO}_1\text{+TA}$ . From the  $251\text{-cm}^{-1}$  band we find the single-phonon energy of the TA and  $\text{TO}_1$  modes to be  $126\text{ cm}^{-1}$  at the zone boundary as compared to  $117\text{ cm}^{-1}$  from the neutron-diffraction measurements.<sup>1</sup> Better agreement between the Raman and neutron-diffraction measurements is obtained at low temperatures where the overlap between adjacent bands is much less. In this case the phonon energy is  $115\text{ cm}^{-1}$  in excellent agreement with the neutron-diffraction measurements.

<sup>25</sup> Indeed, in many crystals, the temperature dependence of the absolute integrated intensity can be used to distinguish between first- and second-order Raman lines. The distinction comes from the fact that the first-order Stokes lines depend on the phonon occupation number as  $(1+n_i)$  whereas the second-order sum bands as  $(1+n_i+n_j+n_k)$ . These occupation numbers vary with temperature as  $[\exp(E_i/kT)-1]^{-1}$ . Unfortunately in  $\text{KTaO}_3$  and  $\text{SrTiO}_3$  the polarization properties also change drastically with temperature. This effect, together with some variation of linewidth and overlap between bands, tends to obscure the dependence of Raman intensity on occupation number and this method of distinguishing first- and second-order Raman lines is not likely to be successful here. For difference combination bands on the Stokes side of the exciting line the intensity goes as  $n_i n_j - n_k$  where  $E_j > E_i$ . In this case, the intensity approaches zero as the temperature is reduced and difference combination bands can easily be distinguished from other Stokes components.

<sup>22</sup> H. Poulet, Ann. Phys. (Paris) **10**, 908 (1955).

<sup>23</sup> R. Loudon, Advan. Phys. **13**, 423 (1964).

<sup>24</sup> L. Rimai, J. L. Parsons, and A. L. Cederquist, Bull. Am. Phys. Soc. **12**, 60 (1967); L. Rimai and J. L. Parsons, Solid State Commun. **5**, 387 (1967). See also D. C. O'Shea, R. V. Kolluri, and H. Z. Cummins, *ibid.* **5**, 241 (1967).

TABLE I. Phonon branch assignments for the second-order Raman spectra and derived single-phonon energies at the Brillouin zone boundary for SrTiO<sub>3</sub> at room temperature.

Second-order energy-shift <sup>a</sup> (cm <sup>-1</sup> )	Assignment	Calculated energy shift <sup>b</sup> (cm <sup>-1</sup> )	Corresponding energy shift in KTaO <sub>3</sub> (cm <sup>-1</sup> )	Derived single-phonon energies at zone boundary		
				Phonon branch	Present work	Published <sup>b</sup> work
81	TO <sub>2</sub> -TA	77	160	TO <sub>1</sub>	126 <sup>d</sup>	117
	TO <sub>2</sub> -TO <sub>1</sub>	77	not seen <sup>c</sup>		114 <sup>d</sup> 130 <sup>d</sup>	
251	2TA	234	123	TA	126 <sup>d</sup>	117
	2TO <sub>1</sub>	234	not seen		114 <sup>d</sup>	
	TO <sub>1</sub> +TA	234	271		130 <sup>d</sup>	
308	TO <sub>2</sub> +TA	311	271	TO <sub>2</sub>	195 <sup>d</sup>	194
	TO <sub>2</sub> +TO <sub>1</sub>	311	not seen		185 <sup>d</sup>	
	TO <sub>4</sub> -TO <sub>2</sub>	350(325) <sup>c</sup>	not seen		211 <sup>d</sup>	
369	TO <sub>4</sub> -TA	427(402) <sup>c</sup>	465	TO <sub>4</sub>	419 <sup>d</sup>	544 <sup>f</sup>
	TO <sub>4</sub> -TO <sub>1</sub>	427(402) <sup>c</sup>	not seen		499 <sup>d</sup>	
	2TO <sub>2</sub>	388	not seen		518 <sup>d</sup>	
629	TO <sub>4</sub> +TA	661(636) <sup>c</sup>	589			
	TO <sub>4</sub> +TO <sub>1</sub>	661(636) <sup>c</sup>	692			
684	2TO <sub>3</sub>	656	not seen	TO <sub>3</sub>	342	328
727	TO <sub>4</sub> +TO <sub>2</sub>	738	738			
1038	2LO <sub>2</sub>	946 <sup>f</sup>	886	LO <sub>2</sub>	516	473 <sup>f</sup>
	2TO <sub>4</sub>	1080 <sup>f</sup>	1095		518	
1325	LO <sub>4</sub> +LO <sub>2</sub>	1280 <sup>f</sup>	not seen			
1618	2LO <sub>4</sub>	1614 <sup>f</sup>	1748	LO <sub>4</sub>	809	807 <sup>f</sup>

A major difference between SrTiO<sub>3</sub> and KTaO<sub>3</sub> is that, at the zone boundary, the TA and TO<sub>1</sub> modes are near degenerate in the former crystal, whereas the TO<sub>1</sub> and TO<sub>2</sub> modes have nearly identical energies in the latter crystal. For this reason, overtones and combination bands involving TA and TO<sub>1</sub> modes are superimposed in SrTiO<sub>3</sub>, whereas this is true for the TO<sub>1</sub> and TO<sub>2</sub> modes in KTaO<sub>3</sub>. Also, the TO<sub>1</sub>-TA band in SrTiO<sub>3</sub> and the TO<sub>2</sub>-TO<sub>1</sub> band in KTaO<sub>3</sub> are not observed since their energy shifts are very close to zero.

The band at 308 cm<sup>-1</sup> is made up of several combination bands, namely the TO<sub>2</sub>+TA band, the TO<sub>2</sub>+TO<sub>1</sub> band, and the TO<sub>4</sub>-TO<sub>2</sub> band. From the TO<sub>2</sub>±TA and TO<sub>2</sub>±TO<sub>1</sub> combinations, we find the TA and TO<sub>1</sub> phonon energies to be 114 cm<sup>-1</sup> and the TO<sub>2</sub> energy to be 195 cm<sup>-1</sup> at the zone boundary. These values are in excellent agreement with the neutron-diffraction values of 117 and 194 cm<sup>-1</sup>. Since the 308-cm<sup>-1</sup> band is made up of both sum and difference combination bands, the band intensity should decrease with temperature but some residual intensity should remain even at very low temperatures. This is qualitatively what is observed. The band at 369 cm<sup>-1</sup> is also a superposition of sum and difference bands and the same remark applies. The 2TO<sub>2</sub> overtone yields a single-phonon energy of 185

cm<sup>-1</sup> in reasonable agreement with the neutron-diffraction measurements.

The bands at 629, 684, and 727 cm<sup>-1</sup> all remain reasonably intense and maintain their band shape even at low temperatures. For this reason, no difference combination bands should be present in this part of the spectrum and we attribute all three of these bands to sum combination bands or overtones. The TO<sub>4</sub>±TA and TO<sub>4</sub>±TO<sub>1</sub> combinations yield single-phonon energies of 499 cm<sup>-1</sup> for the TO<sub>4</sub> mode and 130 cm<sup>-1</sup> for the TA and TO<sub>1</sub> modes at the zone boundary. Infrared measurements give the TO<sub>4</sub> phonon energy as 544 cm<sup>-1</sup> at the zone center, but the energy at the zone boundary is not known. The present measurements indicate that the energy is slightly less than 544 cm<sup>-1</sup> at the zone boundary.

The band at 684 cm<sup>-1</sup> can only be assigned to the 2TO<sub>3</sub> overtone. The single-phonon energy is then 342 cm<sup>-1</sup> for the TO<sub>3</sub> mode in good agreement with 328 cm<sup>-1</sup> from the neutron-diffraction work. This is the only band in either SrTiO<sub>3</sub> or KTaO<sub>3</sub> involving phonons derived from *F<sub>2u</sub>* symmetry.

The addition combination band TO<sub>4</sub>+TO<sub>2</sub> is responsible for the band at 727 cm<sup>-1</sup>. This band, together with the one at 308 cm<sup>-1</sup>, yields phonon energies of 518 and 210 cm<sup>-1</sup> for the TO<sub>4</sub> and TO<sub>2</sub> modes at the zone bound-

ary. Considering the extensive overlap between bands and the superposition of different bands on top of one another, the agreement with the published work is quite good.

The band at  $1038\text{ cm}^{-1}$  is a superposition of the  $2\text{LO}_2$  and  $2\text{TO}_4$  overtones and the band at  $1325\text{ cm}^{-1}$  is the addition combination  $\text{LO}_4 + \text{LO}_2$ . These bands, together with the  $2\text{LO}_4$  overtone at  $1618\text{ cm}^{-1}$ , yield consistent values for the phonon energies of the  $\text{LO}_4$  and  $\text{LO}_2$  modes at the zone boundary. Neutron-diffraction measurements were not made of these modes. Also, it should be noted that the  $\text{LO}_4 + \text{LO}_2$  band is the only combination band found in  $\text{SrTiO}_3$  and  $\text{KTaO}_3$  involving longitudinal modes. The corresponding difference combination band is not seen, but this is not surprising since the sum band is quite weak and the difference band would be reduced in intensity by the Boltzmann factor  $\exp(-E_j/kT) = 0.09$  and would be located in a part of the spectrum where other bands are quite intense. The presence of the  $\text{LO}_4 + \text{LO}_2$  band does show, however, that combination bands involving longitudinal modes are probably just weak in intensity compared to bands involving transverse modes rather than forbidden by symmetry.

### Raman Scattering from Local Modes

As the temperature is decreased, not only do the line shapes of the second-order spectra change but also three new lines appear below about  $110^\circ\text{K}$ . The energy shifts are 39, 148, and  $453\text{ cm}^{-1}$  at  $79^\circ\text{K}$  and 44, 147, and  $449\text{ cm}^{-1}$  at  $24^\circ\text{K}$  (see Fig. 1). The two lowest energy lines are shown in more detail in Fig. 2. These lines appear to be present only in the tetragonal phase below  $110^\circ\text{K}$  and are presumably forbidden by symmetry in the cubic perovskite phase.<sup>26</sup> At first these lines might appear to be first-order Raman spectra from the polar TO modes. Indeed, Schaefele and Weber<sup>27</sup> came to this conclusion and assumed that the tetragonal phase had  $C_{4v}$  symmetry as in  $\text{BaTiO}_3$ . Then, the optical modes would be made up of  $3A_1 + B_1 + 4E$  species, all of which are Raman active.

There are two outstanding reasons to suspect these conclusions. First of all, pure  $\text{SrTiO}_3$  does not become ferroelectric on cooling despite a large increase in dielectric constant. It is unlikely that  $\text{SrTiO}_3$  goes into one of the ferroelectric tetragonal point groups since in that case the crystal would become ferroelectric. It is more likely that it goes into one of the nonferroelectric tetragonal point groups such as  $S_4$ ,  $C_{4h}$ ,  $D_4$ ,  $D_{2h}$ , or  $D_{4h}$ . Second, the energy shifts say at  $79^\circ\text{K}$  do not agree very

well with the known mode energies at the zone center. At  $90^\circ\text{K}$ , Cowley<sup>1</sup> found 42 and  $170\text{ cm}^{-1}$  for the first two polar TO modes from neutron diffraction and Barker<sup>8</sup> gives  $544\text{ cm}^{-1}$  for the other polar TO modes. The difference between these energies and our measured energy shifts is well outside our experimental errors (about  $\pm 5\text{ cm}^{-1}$  on reasonably narrow lines), and the lines appearing below  $110^\circ\text{K}$  are due to Raman scattering from local modes.

Raman scattering is quite sensitive to crystal structure and it is interesting to speculate as to the point group of the tetragonal phase below  $110^\circ\text{K}$ . The absence of first-order scattering in the tetragonal phase is probably due to this process being forbidden by symmetry. Thus, it is likely that the point group of the tetragonal phase in  $\text{SrTiO}_3$  is both nonpolar and has no Raman-allowed single-phonon modes. This is true only of the  $C_{4h}$  and  $D_{4h}$  point groups in the tetragonal system.

### Raman Scattering from Impure $\text{SrTiO}_3$

Since the dielectric properties and lattice dynamics of  $\text{SrTiO}_3$  seemed to be quite sensitive to impurities, we investigated one sample which contained some impurities. Our hope was that the crystal structure of the phases at low temperatures would be different from that of the pure  $\text{SrTiO}_3$  and that first-order Raman scattering might be allowed in one of these phases.

As stated above, the impure and pure samples give identical spectra at room temperature. As the impure sample is cooled, three lines appear as in the pure sample but the lines are located at different energy shifts. The close agreement between the energy shifts shown in Fig. 3 and the known energies of the polar TO modes at the zone center (see above) make it practically certain that these lines are first-order Raman spectra from the polar TO modes. Further, scattering from the local modes is apparently forbidden in this phase. Unfortunately, there are several obstacles which make it difficult to determine the point group in this phase which we assume is in the tetragonal system. First, it is not known if the impure  $\text{SrTiO}_3$  is ferroelectric at  $78^\circ\text{K}$ . Second, although the crystal is aligned as described above, the tetragonal axis may be oriented along any one of the  $\langle 100 \rangle$  directions and is probably randomly oriented along all three orthogonal  $\langle 100 \rangle$  directions. Third, neither the longitudinal nor the  $E$  modes are seen. Nevertheless, a reasonable guess can be made as to the point group of the tetragonal phase. First of all, it cannot be  $C_{4h}$  or  $D_{4h}$  since no first-order Raman would be allowed in  $\text{SrTiO}_3$  with this point group. Second,  $D_{2d}$  and  $D_4$  do not have any Raman-active modes with diagonal scattering elements. Of the three remaining point groups in the tetragonal system ( $S_4$ ,  $C_4$ , and  $C_{4v}$ ), the experimental data are most consistent with the  $C_{4v}$  symmetry but the other point groups cannot be eliminated without having a single domain crystal with the tetragonal axis in a known direction.

<sup>26</sup> However, there is some evidence of scattering from local modes even in the cubic phase as evidenced by the small bump that appears on the low-energy side of the  $78\text{-cm}^{-1}$  mode in Fig. 2. This mode decreases in energy as the temperature is decreased and is especially evident at  $112^\circ\text{K}$ . We believe that this is a local mode associated with the ferroelectric TO mode but with a different energy.

<sup>27</sup> R. F. Schaefele and M. J. Weber, J. Chem. Phys. **46**, 2859 (1967).



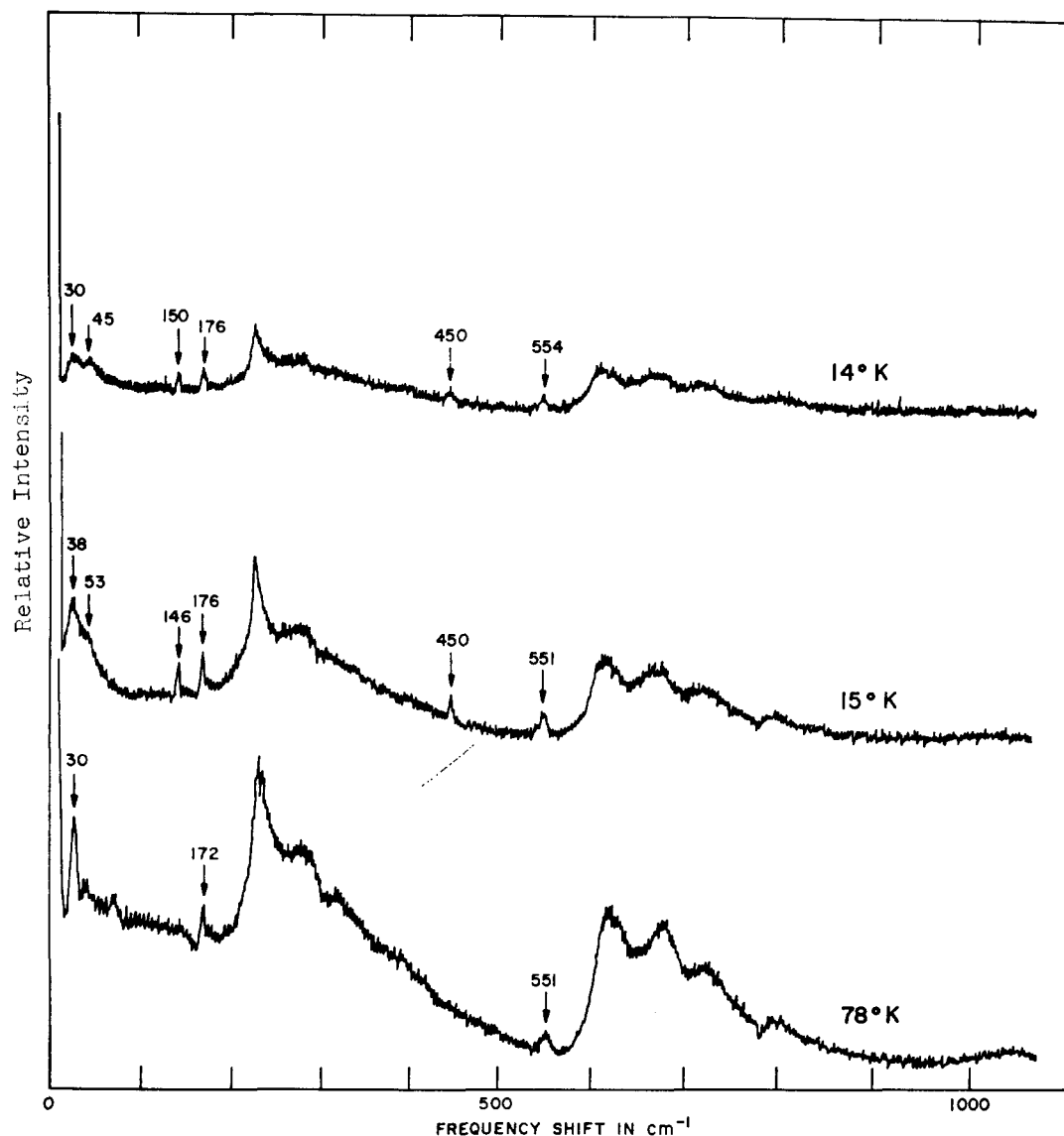


FIG. 3. The Raman spectrum of the dark, somewhat impure sample of  $\text{SrTiO}_3$  using the 5145-Å laser line.

As the temperature is reduced below 78°K, the impure sample undergoes further phase transitions presumably into crystal structures with lower symmetry than the tetragonal system. What is instructive is the fact that both the first-order spectra and the scattering from local modes are present simultaneously in the same spectrum (see spectra at 15° and 14°K in Fig. 3). This demonstrates that the three lines found in pure  $\text{SrTiO}_3$  at low temperatures cannot be first-order Raman lines.

### CONCLUSIONS

The Raman spectrum of  $\text{SrTiO}_3$  at room temperature is entirely second order in agreement with the selection rules for the cubic perovskite structure. The peaks in the spectrum originate largely from pairs of transverse-polarized phonons with wave vectors near the zone

boundary although one LO combination and two LO overtones are observed. It appears likely that other combinations and overtones are hidden under the more intense spectra from the polar TO and TA modes. Also, the absence of certain combinations and overtones is more likely due to weak scattering compared to the observed spectra rather than restrictions from selection rules. The Raman spectrum of  $\text{KTaO}_3$  and  $\text{SrTiO}_3$  at room temperature are closely related in that the same combinations and overtones tend to give intense peaks. The different appearance of the two spectra is due largely to the different dispersions of the phonon branches in the two crystals. For example, in  $\text{KTaO}_3$  at the zone boundary the TA mode is at about 60  $\text{cm}^{-1}$  and the  $\text{TO}_1$  and  $\text{TO}_2$  modes at about 200  $\text{cm}^{-1}$ . For this reason the spectra of  $\text{KTaO}_3$  are largely dominated by sum and difference combination

pairs separated by twice the TA energy and combinations involving the  $\text{TO}_1$  and  $\text{TO}_2$  modes usually overlap. Also, the lowest-energy peak is a TA overtone which remains intense even at low temperatures. In contrast, the TA and  $\text{TO}_1$  modes of  $\text{SrTiO}_3$  are near degenerate at the zone boundary with energy  $117\text{ cm}^{-1}$  and the  $\text{TO}_2$  mode has an energy of  $194\text{ cm}^{-1}$ . Because of the higher TA energy, the spectra appear to consist of groups of peaks rather than combination pairs. One higher-energy group around  $600$  to  $750\text{ cm}^{-1}$  is temperature insensitive and consists of sum combination bands, and the lower-energy group around  $300$  to  $400\text{ cm}^{-1}$  is partially temperature sensitive and consists of difference combination bands together with some overlapping sum bands. The differences between the  $\text{KTaO}_3$  and  $\text{SrTiO}_3$  spectra are due to phonon energy differences at the zone boundary rather than drastic changes in the scattering efficiencies or selection rules.

The three sharp lines which appear in the pure sample below the  $110^\circ\text{K}$  phase transition are attributed to scattering from local modes. These lines do not have the same energies as the polar TO modes. Also, in an im-

pure  $\text{SrTiO}_3$  sample at low temperatures, Raman scattering is found from both the local modes and the polar TO modes. The absence of ferroelectricity and first-order Raman scattering in the tetragonal phase makes it probable that the point group of this phase is  $C_{4h}$  or  $D_{4h}$ . The impure  $\text{SrTiO}_3$  undergoes different types of phase transitions as the sample is cooled to liquid-helium temperatures. This is clearly seen in the different spectra observed at low temperatures and illustrates how sensitive Raman scattering is to crystal symmetry. The point group of the impure sample at  $78^\circ\text{K}$  is either  $S_4$ ,  $C_4$ , or  $C_{4v}$  with the latter most likely. At lower temperatures the symmetry is undoubtedly lower than tetragonal.

#### ACKNOWLEDGMENTS

We wish to thank S. Singh and J. E. Geusic for reading the manuscript, A. M. Johnson and D. MacNair for assistance with the argon-ion laser, and M. A. Karr and J. R. Potopowicz for their excellent technical assistance. We also wish to thank C. H. Perry and A. Linz for a sample of  $\text{SrTiO}_3$ .

## Electronic Absorption Spectra of Methanal Azine and the Methyleniminyl Free Radical

J. F. OGILVIE\* AND D. G. HORNE†

*University of Cambridge, Department of Physical Chemistry, Lensfield Road, Cambridge, England*

(Received 31 July 1967)

The methyleniminyl free radicals,  $\text{H}_2\text{CN}$ ,  $\text{HDCN}$ , and  $\text{D}_2\text{CN}$  have been produced from flash photolysis of their stable dimers, the methanal azines  $\text{H}_2\text{CNNCH}_2$ ,  $\text{HDCNNCHD}$ , and  $\text{D}_2\text{CNNCD}_2$ . The electronic absorption spectra of both radicals and parent substances are presented and discussed in terms of simple molecular orbital descriptions of the transitions. The photochemical processes are related to these transitions, and applications to the corresponding hydrocarbon diene, butadiene-1,3, are noted.

A brief report<sup>1</sup> has already summarized some principal results concerning the participation of methanal azine,  $\text{H}_2\text{C}=\text{N}=\text{N}=\text{CH}_2$ , in the photodecomposition of diazomethane in cryogenic matrices. It was stated that methanal azine (previously termed formaldazine), formed by the combination of methylene radicals with diazomethane, was subsequently photolyzed to produce methylenimine and hydrogen cyanide, via the disproportionation reaction of a pair of methyleniminyl ( $\text{H}_2\text{C}=\text{N}$ ) radicals.

The evidence cited for the discrete existence of the  $\text{H}_2\text{CN}$  radicals in that reaction consisted of the direct detection of an absorption spectrum, in the ultraviolet, assigned to an electronic transition of this species after flash photolysis of methanal azine in the gas phase.

The same spectrum has also been observed during the flash photolytic decomposition of gaseous methanal oxime,  $\text{H}_2\text{C}=\text{NOH}$ .<sup>2</sup> Absorption bands at similar wavelengths have also been obtained during the flash photolysis of both ethanal azine,  $\text{CH}_3\text{CH}=\text{N}=\text{N}=\text{CHCH}_3$ , and propanone azine,  $(\text{CH}_3)_2\text{C}=\text{N}=\text{N}=\text{C}(\text{CH}_3)_2$ .<sup>2</sup> Thus methyleniminyl would seem to be the first member of a new homologous series of free radicals, of which the near-ultraviolet electronic transitions are conveniently situated to be employed for monitoring concentrations during investigations of their reaction kinetics.

Methanal azine is itself of some interest in that its electronic absorption spectrum is comparable to that of butadiene-1,3, its hydrocarbon analogue. Like butadiene, methanal azine is the first member of a series of conjugated acyclic dienes, but the nitrogen atoms present in the azines confer special properties on these molecules. Further members of this series have been

\* Research Fellow of Emmanuel College, Cambridge, 1963-66. Present address: Department of Chemistry, Memorial University, St. John's, Newfoundland, Canada.

† Present address: Department of Chemistry, University of Alberta, Edmonton, Canada.

<sup>1</sup> J. F. Ogilvie, *Chem. Commun.* **1965**, 359.

<sup>2</sup> D. G. Horne and R. G. W. Norrish (to be published).